ADVANCED FUNCTIONAL MATERIALS
www.afm-journal.de

Ionic Skin with Biomimetic Dielectric Layer Templated from *Calathea Zebrine* Leaf

*Zhiguang Qiu, Yongbiao Wan, Wohua Zhou, Jingyi Yang, Junlong Yang, Jun Huang, Jianming Zhang, Qingxian Liu, Siya Huang, Ningning Bai, Zhigang Wu, Wei Hong, Hong Wang, and Chuan Fei Guo**

Flexible electronic skins (e-skins) with high sensitivity and broad-range pressure sensing are highly desired in artificial intelligence, and human–machine interaction. Capacitive-type e-skins have a simple configuration, but the change in dimensions of the dielectric layer is often quite limited, although introducing surface microstructures might improve the sensitivity in some extent. Moreover, such surface structures typically require costly microfabrication methods to fabricate. Here, a low-cost microstructured ionic gel (MIG) with uniform cone-like surface microstructures for high-performance capacitive e-skins is reported. The MIG film is templated from a *Calathea zebrine* leaf using soft lithography, and sandwiched by two flexible electrodes. The device exhibits a low limit of detection down to 0.1 Pa, a ultrahigh sensitivity of 54.31 kPa^{-1} in the low pressure regime (<0.5 kPa), and the sensitivity keeps larger than 1 kPa^{-1} over a broad-range pressure from 0.1 Pa to 115 kPa. Electric double layers (EDL) form on both the top and bottom interfaces, and the area of EDL of the rough interface increases as the cones are compressed. Such ionic skins with biomimetic gel templated *Calathea zebrine* leaf allow for sensitive tactile sensing in the applications of human–machine interaction.

1. Introduction

The emerging field of electronic skins (e-skins) has significantly promoted the progress of artificial intelligence, human–machine interaction, health monitoring, and soft robots.[1–8] For example, the so-called "co-robots" are expected to have the ability to friendly interact with human beings, the environment, and other robots,[9] and the interactions require e-skins that are lightweight, flexible, and highly sensitive to the touch. Especially, home service robots and artificial limbs are required to communicate with human beings via friendly human–machine interaction. An e-skin is expected to perform like the human skin, which feels tactile pressure in a broad range from light touches (0–10 kPa, low-pressure regime) to object handling levels (10–100 kPa, medium-pressure regime).[1,4] The key quality parameters of an e-skin include sensitivity, limit of detection (LOD), response time, and durability.[4] There is still a long way to enhance the sensitivity and broaden the sensing pressure of flexible e-skins. For instance, many reported flexible e-skins exhibited a saturated response in medium-high pressure regime, leading to poor discrimination.[10] There are typically four types of e-skins based on the sensing mechanism, including resistive,[11–13] capacitive,[14–16] piezoelectric,[17–19] and triboelectric types.[20,21] Particularly, capacitive e-skins present advantages of simple device construction, fast response time, low power consumption, and higher sensitivity than other sensors, and are thereby widely explored.[5,22] A capacitive e-skin is typically in framework of two parallel electrodes that sandwich

Z. Qiu, Y. Wan, J. Yang, Dr. J. Yang, J. Huang, Prof. J. Zhang, Q. Liu, Prof. S. Huang, N. Bai, Prof. Z. Wu, Prof. H. Wang, Prof. C. F. Guo
Department of Materials Science and Engineering
Southern University of Science and Technology
Shenzhen 518055, China
E-mail: guocf@sustc.edu.cn
Y. Wan, J. Huang
School of Materials Science and Engineering
Harbin Institute of Technology
Harbin 150001, China
W. Zhou
Kingfa Science and Technology Co., Ltd
Guangzhou 510000, China
The ORCID identification number(s) for the author(s) of this article can be found under https://doi.org/10.1002/adfm.201802343.
Prof. J. Zhang, Prof. S. Huang
Academy for Advanced Interdisciplinary Studies
Southern University of Science and Technology
Shenzhen 518055, China
Prof. Z. Wu
State Key Laboratory of Digital Manufacturing Equipment and Technology
Huazhong University of Science and Technology
Wuhan 430074, China
Prof. W. Hong
Department of Mechanics and Aerospace Engineering
Southern University of Science and Technology
Shenzhen 518055, China

DOI: 10.1002/adfm.201802343

a dielectric layer. An external force applied to the capacitive e-skin will change the thickness of the dielectric layer and thus lead to the variation in capacitance, but the achieved sensitivity of the sensors is typically very low due to the relatively limited change in thickness or area of the dielectric layer. Dielectrics with microstructures that can be easily compressed, such as porous or hollow structures,[10,23] micropyramids arrays,[1] and microspheres arrays,[15] are helpful to improve the sensitivity. Tactile sensors with biomimetic microstructured electrodes templated from lotus leaf have also been reported.[15] However, still few capacitive e-skins with microstructured dielectric layer exhibit a sensitivity over 10 kPa^{-1}, and the sensitivity significantly decreases at high-pressure range.[6,24]

In the year 2012, Pan and coworkers found that ionic liquid (IL) showed ultrahigh capacitance to pressure sensitivity because charges of different signs in the electric double layer (EDL) is on atomic scale.[25] Ionic gel senses like IL and behaves like elastomers mechanically. Recently, ionic gels of polymer composites have drawn increasing attentions and the devices exhibit high specific capacitances.[26–28] For gate dielectric layer of a free-standing ionic gel, the specific capacitance could reach up to 10 $\mu F \cdot cm^{-2}$ at low frequencies.[26] Very recently, a flexible capacitive skin with a new record of maximum sensitivity 41.64 kPa^{-1} was obtained based on micropyramidal ionic gels by taking advantages of microstructures and the special sensing mechanism of ionic gel.[28] However, such microstructures are typically made by using photolithographic routes and come at a high price. On the other hand, high order and high precision of the lithographic microstructures are not necessarily required to yield high performances. It is therefore reasonable to find a cost-effective way to make microstructured ionic gels (MIGs) which might significantly improve the sensitivity of flexible e-skins.

Here, we report a MIG film and use this film as a dielectric layer in flexible ionic skins. The MIG film is templated from the *Calathea zebrine* leaf to form surface microcones with an average height of ≈25 µm and an intercone distance of ≈34 µm, being an alternative to the micropyramids fabricated by using photolithographic processes or anisotropic etching. *Calathea zebrine* leaves have highly uniform surface microstructures, but are seldom studied for biomimetic applications probably because the surface is not superhydrophobic.[29] Compared with conventional microfabrication methods, templating ionic gel from a *Calathea zebrine* leaf is cost-effective and environmentally friendly. The flexible MIG-based skin exhibits a fast response time within 29 ms, an LOD as low as 0.1 Pa, and a high sensitivity of 54.3 kPa^{-1} in the ultralow pressure regime (<0.5 kPa). Significantly, the sensitivity keeps larger than 1 kPa^{-1} over a broad range from 0.1 Pa to 115 kPa (higher than one atmosphere), and the normalized change in capacitance achieves 545 (or capacitance achieves 5466 pF), which is much higher than existing results.[28] The flexible MIG-based skin also shows high robustness: it is compressed for at least 5400 cycles without showing fatigue. The high performance lies in the remarkable ionic-electric capacitive interfaces, which offers significant higher change in capacity than normal capacitive e-skins. This work also gives detailed sensing mechanism: EDL forms at the cone-tip/electrode interface; and upon compression, the capacitance to pressure response lies in the change in the interfacial area of the EDL capacitors in parallel. That is, the contact area of the microstructured surface determines the response. We have also used finite-elemental analysis (FEA) to simulate sensing process. We demonstrate that the ionic skin can be used in the application of spatial pressure identification and human–machine interaction. This work opens a new path to utilize structures from natural materials to enhance the performance of ionic skins.

2. Results and Discussion

2.1. Preparation and Characterization

Figure 1a shows the fabrication and the structures of the flexible MIG-based skin. The ionic gel uses a blended solution of poly(vinylidene fluoride-co-hexafluoropropylene) (P(VDF-HFP)) as the structuring polymer and 1-ethyl-3-methylimidazolium bis(trifluoromethylsulfonyl)imide ([EMIM][TFSI]) as the IL. The microstructures in ionic gel surface were made by using a low-cost templating method, which is a type of soft lithography.[30] Figure S1 in the Supporting Information displays an optical microscopy and a scanning electron microscopy (SEM) image of the *Calathea zebrine* leaf, which shows relatively uniform microstructures with cone-like morphology. After the first molding of the original *Calathea zebrine* template, the molded pattern is replicated again by spinning the blended solution of ionic gel onto the second template. An ionic gel film with array of microcones that precisely replicate the leaf surface is formed after peeling off, being used as the active dielectric layer (Figure S2, Supporting Information). This templating process presents several advantages over traditional microfabrication methods. First, it is an environmentally friendly method that does not involve in toxic chemicals such as etchants and organic solvents. Second, this method is fast, and it well replicates the surface structures of the natural material. Third, the natural template is easily available and the process is cost-effective. The flexible electrode with a low sheet resistance (R_{sq}) below 10 $\Omega \cdot sq^{-1}$ was fabricated via spraying AgNWs onto a colorless polymide (CPI) substrate as shown in Figure S3 in the Supporting Information. The device consists of the MIG dielectric and two electrodes in framework of CPI/AgNWs/MIG/AgNWs/CPI.

Figure 1b displays a SEM image of the second template molded from a *Calathea zebrine* leaf. The average diameter of the caves is about 35 µm from the random statistical distribution. After plasma treatment and second templating, relatively uniform microcones of ionic gel with and a height of ≈25 µm and intercone distance of 34 µm were replicated as shown in Figure 1c, d and Figure S4 in the Supporting Information. It should be noted that the microstructures at different locations on the leaf surface are not fully consistent. The main difference comes from the leaf edge, and the microstructures are basically consistent when cutting away the edges. This can still give rise to a relatively uniform template with a typical size of 5 cm × 10 cm, which can already fulfill with many applications. The as-fabricated MIG film (Figure S5a, Supporting Information) and the second polydimethylsiloxane (PDMS) template (Figure S5b, Supporting Information) are not transparent on account of the

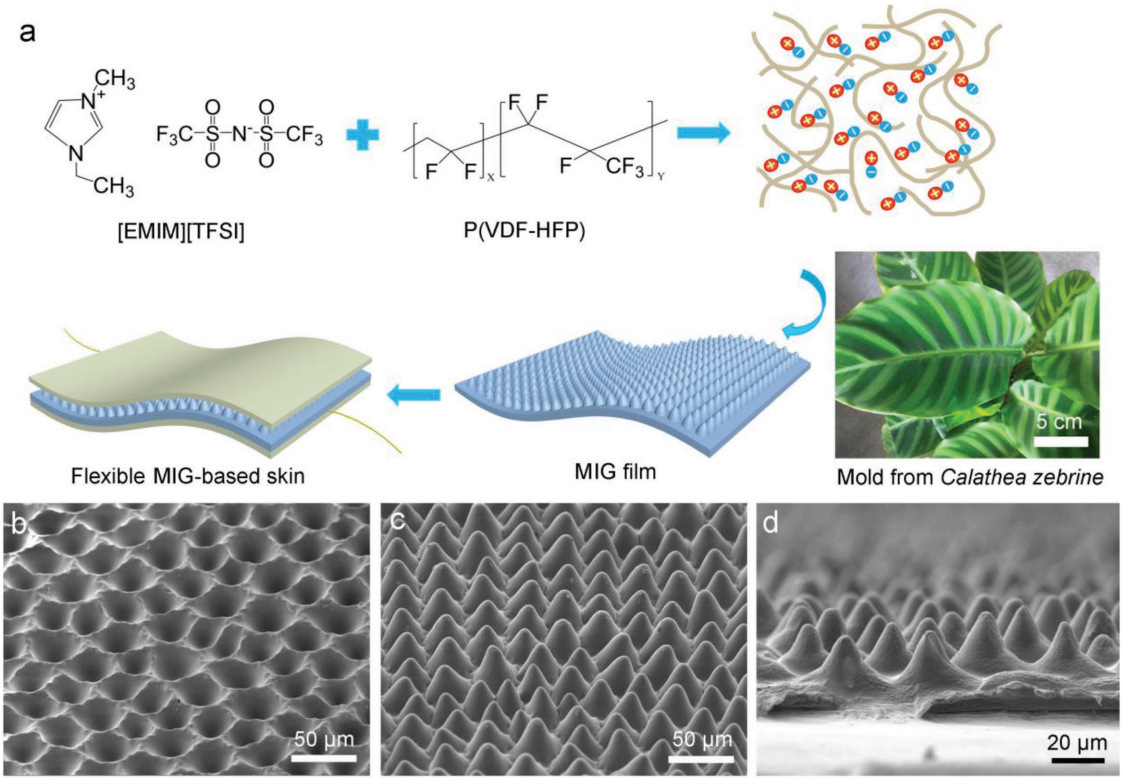

Figure 1. Fabrication of flexible MIG-based skin. a) Schematic illustration of the fabrication of a mechanically flexible capacitive sensor with an MIG dielectric layer. The cross-sectional scheme of the sensor depicts the molecular structures of the matrix and the IL: [EMIM][TFSI] and P(VDF-HFP). The sensor consists of CPI/AgNWs/MIG/AgNWs/CPI multilayers. b) 45° tilt view SEM image of the molding template. c) 45° tilt view and d) cross-sectional morphology of the MIG film.

light scattering caused by the microstructures. Significantly, the second PDMS template can be reused for at least several times and the MIG films in different cycles of molding still maintain the morphology and features, as shown in Figure S6 in the Supporting Information.

2.2. Basic Sensing Properties

The sensing properties of the flexible capacitive skin are evaluated in **Figure 2**. Considering that the subtle pressure generated by gentle finger touch and low–medium pressure caused by daily motion are ranging from 0 to 10 and 10 to 100 kPa, respectively,[4] the tested pressure range is set to cover the pressure range of 0–115 kPa. The pressure applied on the device was swept from 0 to 115 kPa controlled by a force gauge, and corresponding changes in capacitance were continuously measured and plotted against time. By plotting each applied pressure and maximum capacitance response point by point, the change ratio of capacitance as a function of applied pressure is shown in Figure 2a. The sensitivity of the flexible MIG-based skin is given by the equation $S = \delta(\Delta C/C_0)/\delta P$, where C_0 is the initial capacitance, ΔC is the relative change of capacitance (C–C_0), and P is the applied pressure. The initial capacitance C_0 of the device is ≈10 pF at a test frequency of 1 MHz. The capacitance increases with the decreasing of frequency (Figure S7, Supporting Information), a characteristic of ionic-type sensor. By differentiating the curve or depicting the tangent of the curve, we are able to calculate the sensitivity of the skin. It shows that the capacitance responses have four different stages depending on the compressive pressure. In the first stage, a high sensitivity of 54.31 kPa^{-1} (inset of Figure 2a) was observed at an ultralow pressure range (<500 Pa). The second stage from 500 Pa to 10 kPa exhibits a linear sensing behavior with a high sensitivity of 30.11 kPa^{-1}. In the third stage (10–40 kPa) and fourth stage (40–115 kPa), the sensor exhibits average sensitivities of 8.42 and 1.03 kPa^{-1}, respectively. To evaluate the LOD of the MIG-based skin, pressures with a 0.1 Pa increment (the highest resolution of the force gauge) were loaded to the device. As shown in Figure 2b, capacitance of the MIG-based skin could accurately respond to the ultralow pressure with a quite similar waveform, and an LOD of 0.1 Pa was confirmed. Compared with the reported results of capacitive e-skin in literature[1,10,28,31,32] (including those with microstructure ionic gel made by conventional microfabrication), our device shows higher sensitivity all over the pressure range from 0.1 Pa to 115 kPa, as shown in Figure 2c. Specifically, the sensitivity of 54.31 kPa^{-1} (in low pressure < 500 Pa) is higher than that of any existing capacitive e-skins to our best knowledge. Note that many reported e-skins were not able to distinguish in the medium- to high-pressure regime (>50 kPa) due to the saturated response. Here our sensor still exhibits a high sensitivity of 1.03 kPa^{-1} in the pressure regime of 40–115 kPa, which is 100 times higher than the results in literature.[15,23,33,34]

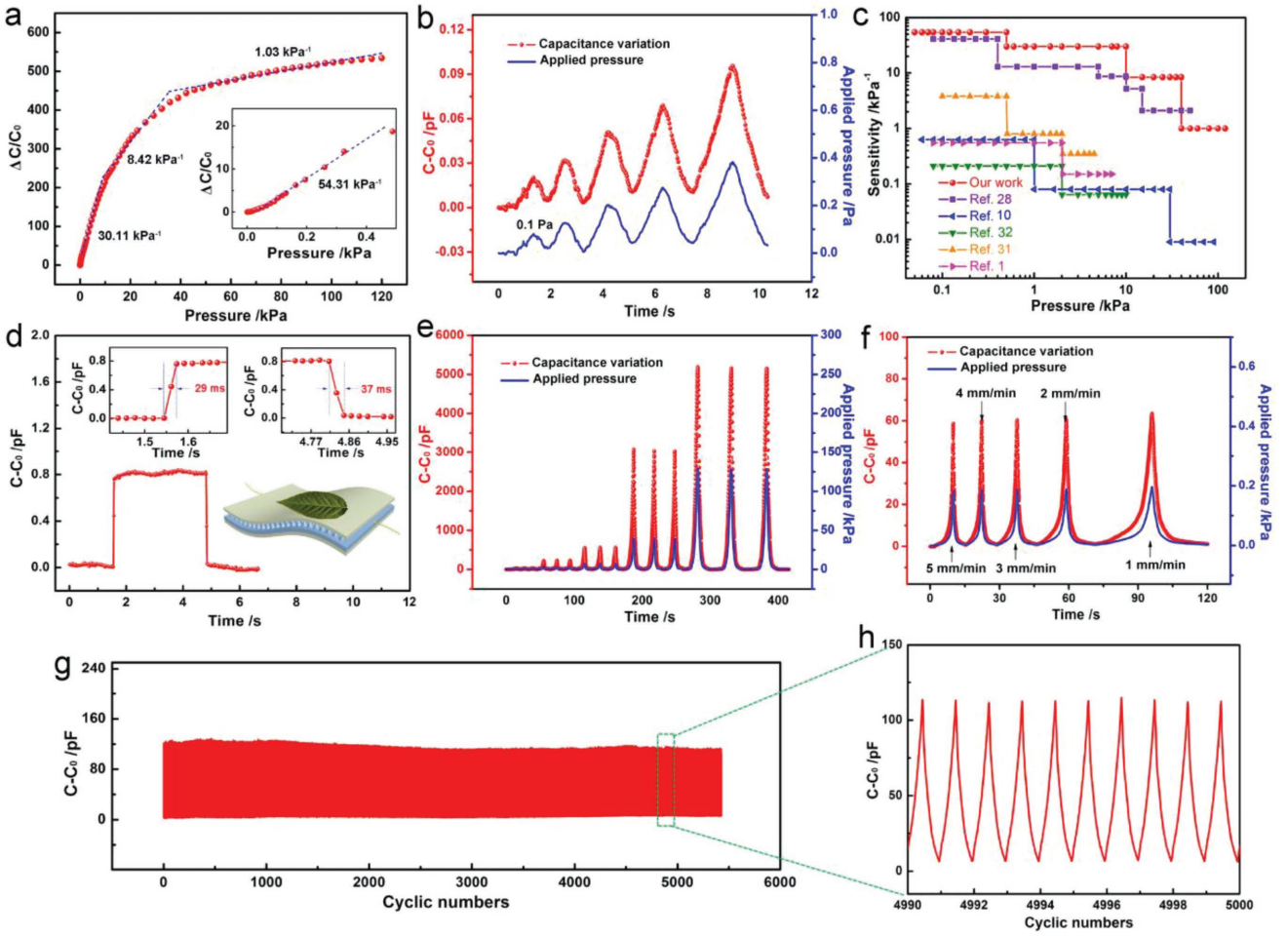

Figure 2. Sensing performance of flexible MIG-based skin. a) Change in capacitance as a function of pressure in the pressure regime from 0.1 Pa to 115 kPa. b) Capacitance changes with pressures from 0.1 to 0.4 Pa. c) Comparison of the sensitivity of our skin with previous reported results. d) Pressure response of the sensor to a myrcia placed on the top of the sensor, insets shows response and recovery time. e) Capacitance signals at pressures of 2, 6, 40, and 115 kPa, indicating high repeatability. f) Capacitance variations at different loading speeds at 0.2 kPa. g) Working stability of the sensor tested for 5400 cycles under a pressure of 0.3 kPa. h) The recorded capacitance variations from 4990 to 5000 cycles.

To investigate the response time of the e-skin, a myrcia (about 20 mg) was carefully loaded on the top surface of the device (Figure 2d). The capacitance of the device rapidly ascended within 29 ms, which exceeds the response speed of human skin (30–50 ms),[35] and then the capacitance maintained at a stable value. After removing the myrcia, the capacitance of the device promptly recovered to the initial value in about 37 ms (the inset of Figure 2d). Furthermore, we also tested real-time responses of the device with loading/unloading pressures of 2, 6, 40, and 115 kPa for three cycles at each pressure (Figure 2e). The results show that the flexible MIG-based skin presents stable responses with high repeatability. Not only that, the device was also able to respond to the continuous pressure with different loading speeds (1–5 mm·min^{-1}), and produced an excellent match between the pressure and the capacitance with stable, continuous, clean, and highly reproducible signals at various pressures, as shown in Figure 2f. All these real-time tests indicate that the flexible skin possesses the potential for dynamic consecutive pressure detection. To investigate the mechanical durability of the MIG-based skin, the device was subjected to 5400 compression/release cycles at a repeated pressure of ≈0.3 kPa (Figure 2g), exhibiting no fatigue. Figure 2h shows that no drift of the responses was found, and the single waves from the 4990th to the 5000th compression/release cycles keeps exactly the same amplitude and waveform, thus confirming high reproducibility and durability of the MIG-based skin.

The capacitance response of ionic-type devices can often be affected by the temperature and humidity. Here because the ionic dielectric layer is sealed, we found that the device is basically stable under different humidity (5%, 55%, and 95%, see Figure S8a, Supporting Information). However, the device shows significant differences in response to different temperatures of 25, 37, and 50 °C (Figure S8b, Supporting Information), although the response is stable when keeping at a given temperature. The result indicates that sometimes the device is required to be calibrated to eliminate the influence of temperature. The capacitance response to pressure also shows hysteresis, and the hysteresis loops almost overlaps over a few cycles (Figure S9, Supporting Information).

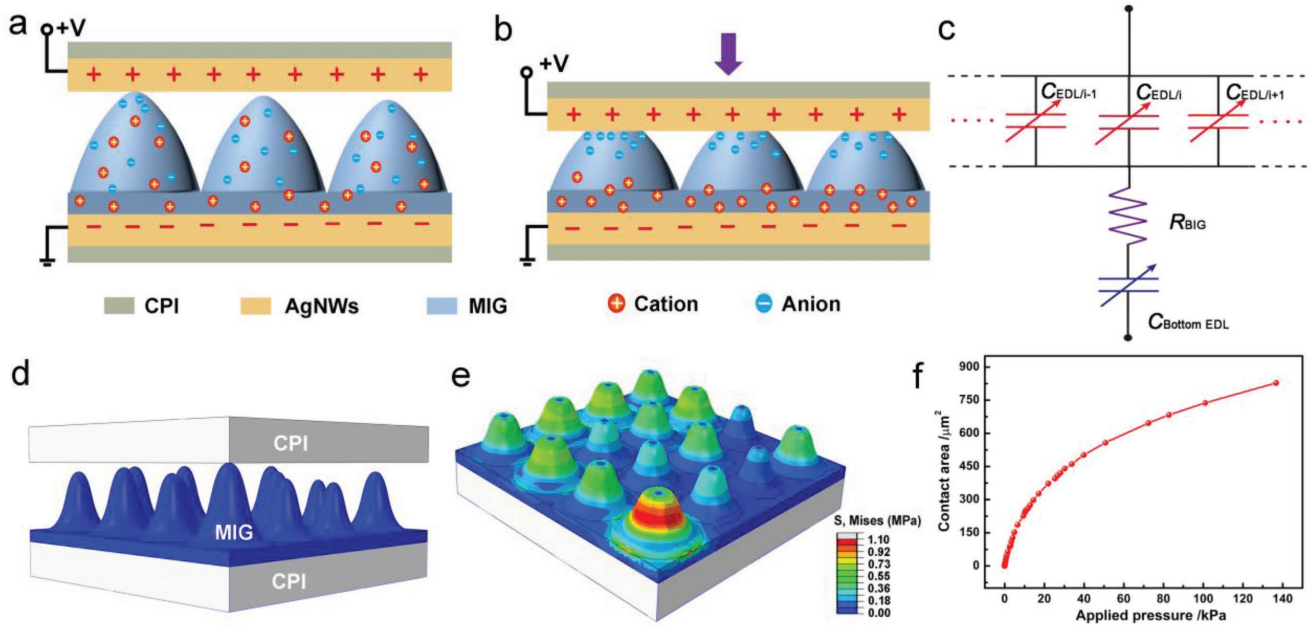

Figure 3. Sensing mechanism of MIG-based skin. a,b) Graphical explanation of the sandwiched structure and charge distribution in the sensor (a) before and (b) under loading. c) Equivalent electrical circuit of the sensor. d) The FEA simulation model of microcones with statistical distribution in Figure S4b. e) Stress distribution of the microcones under an applied pressure of 100 kPa. f) The contact area between the microcones and opposing electrode as a function of applied pressure, showing a wide sensing range beyond 100 kPa.

2.3. Sensing Mechanism

The bionic microstructures and electrical properties of the ionic gel play critical roles to the high performance of the MIG-based skin. As illustrated in **Figure 3**a, there are massive low molar positive and negative charged ion pairs distributed in the MIG film. Unlike the traditional flexible electrostatic capacitive e-skins, the MIG-based skin primarily utilizes a remarkably ionic-electronic capacitive interface, or EDL.[36] Electrons on the electrode and the counter ions in the MIG film accumulate and attract to each other at a nanometer distance, which leads to an ultrahigh specific capacitance.[37] The EDL capacitance is essentially proportional to the area of the ionic-electronic contact at a given temperature. At the unloading state, only a few microcones of the MIG film contact with the electrode resulting in a low initial capacitance. When loading a pressure, the contact area of the interface increases, and some shorter cones begin to touch with the electrode. As a result, the EDL area significantly increases and capacitance also increases accordingly (Figure 3b). According to the Gouy–Chapman–Stern model, this interface without electrochemical reaction can be simply modeled as a capacitive element.[38] The capacitance of the bottom flat interface keeps almost constant and is much larger than that of the top interface. Figure 3c shows an equivalent circuit of the device. For capacitors in series, the total capacitance C is given by $1/C = 1/C_{top}+1/C_{bottom}$, where C_{top} and C_{bottom} denotes the capacity of the top and bottom interfaces, respectively. C_{bottom} is typically much larger than C_{top}, thus the term $1/C_{bottom}$ contributes little to the total capacitance and can be ignored. Therefore, the sensitivity of the device is largely contributed by the rough surface. Here, the top EDL capacitances are in parallel to form one top EDL capacitance ($C_{top} = \Sigma C_{EDL/i}$), determined by the number of cones that touch the top electrode and the contact area for each cone. It should be noted that the microcones are in the elastic regime under the pressure region from 0.1 Pa to 115 kPa. Our SEM observation indicates that the cones still keep the original morphology after being subjected to 115 kPa (Figure S10, Supporting Information). The large elastic limit is important to the stability of the sensor.

To understand the sensing mechanism of the MIG-based skin, FEA that simulates the area of ionic-electronic contact against external load was conducted, as shown in Figure 3d–f. More details of the FEA simulation can be found in Table S1 and Figure S11–S13 in the Supporting Information. In the model, the heights of the cones were selected based on our SEM observation with near normal distribution of 25 ± 4 μm (Figure S4, Supporting Information). Only the highest cone contacts with the top electrode in the initial status (Figure 3d). Upon pressing, local stress is concentrated at the cone tips to squeeze contacted cones, and shorter cones start to contact with the electrode as the displacement increases (Figure 3e). The contact area increases as more cones get contacted with the electrode and the contact area of each cone increases. For EDL, the capacitance is in direct proportion to the contact area. Figure 3f displays the contact area as a function of applied pressure (1–140 kPa), showing a curve similar to the $\Delta C/C_0$–P curve shown in Figure 2a. That is, the sensitivity is higher at the beginning and decreases as pressure increases. The FEA result shows that the cone structure still sensitively responds to the pressure beyond 100 kPa, in accordance with the experimental data, and the wide pressure range of sensing is seen for both distributed and uniform cone height (Figure S13, Supporting Information).

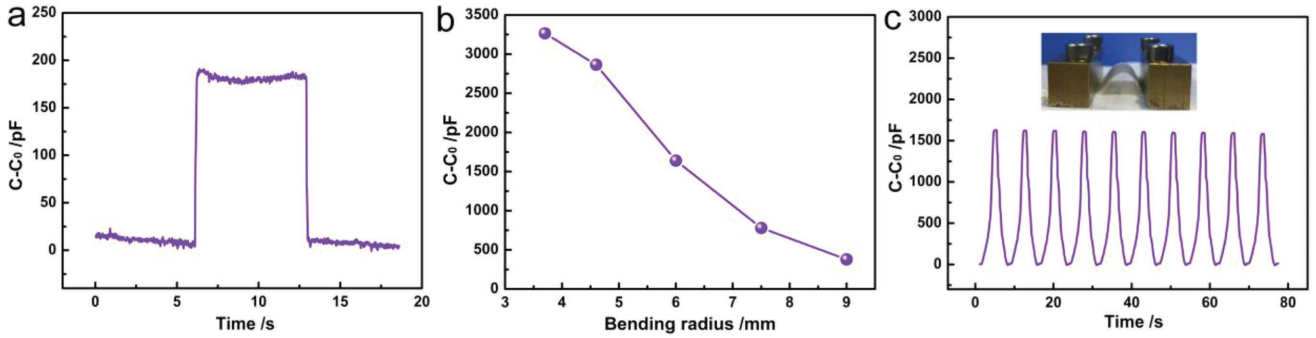

Figure 4. Sensing properties of the MIG-based e-skin under bending. a) Static bending sensing with a 10 mm bending radius. b) Capacitance response as a function of bending radius. c) Cyclic dynamic bending sensing with a bending radius of 6 mm.

The MIG is important to the high sensitivity and the fast response. Compared with the MIG-based device, the device with a flat ionic gel exhibits a maximum sensitivity of only ≈1 kPa^{-1} and a response time of ≈200 ms (Figure S14a–c Supporting Information), while the device using microstructured electric layer with no IL exhibits an even lower maximum sensitivity of 0.64 kPa^{-1}, which is 84 times smaller than that of the MIG-based skin (Figure S14d, Supporting Information). The result confirms that the high performance of the MIG-based skin is contributed by both the microstructures and the ionic gel. Apart from the MIG, the density of AgNWs electrode also influences the sensing performance of the ionic skin. Higher density of the AgNWs does not obviously affect the initial capacitance, but leads to larger EDL area and therefore stronger response upon compression (see Figure S15, Supporting Information).

Surface microstructures have been used as the dielectric layer in flexible tactile sensors to make the compression more easily than a flat dielectric and thus to improve the sensitivity.[1,15] However, for direct capacitance, the enhancement of sensitivity stems from the change in thickness and resulting change in permittivity, which are often limited. Here, the microcones play a quite different role. The compression will lead two changes: the height of the cones, and the area of the EDL capacitors in parallel. It is the change in EDL interfacial area other than height that reflects the change in capacitance, and only the rough surface of the MIG contributes to the sensing. Therefore, the design of the microstructures for EDL-type skins will be different from that of common capacitive-type e-skins. For example, common direct-capacitive-type e-skins prefers sparse and high-aspect ratio surface microstructures to achieve a high sensitivity,[39,40] but judged from the sensing mechanism that only the contact area matters, this strategy will lead to weak response for the EDL-type skins.

2.4. Bendability of the Device

The flexibility of the device is important to its applications. The ionic skin was subjected to static bending, and dynamic bending at different bending radii. Under static bending at a bending radius of 10 mm, the signal is generally stable at the bending status and returns to the initial value as the device goes to the non-bent status (**Figure 4**a). The capacitance response is also sensitive to the bending radius. Figure 4b shows that the signal increases as bending radius decreases from 9.0 to 3.6 mm under dynamic bending. At a given bending radius, the signal is found to be quite stable after a few bending cycles (Figure 4c). The response to bending can be understood by analyzing the deformation of the cones. For a sandwiched structure, bending will cause in-plane tensile and compressive stresses, respectively, on both sides of the neutral axis. However, the normal stress is always compressive, and increases as the bending radius decreases, leading to increased contact area of the cones and thereby stronger response. Based on the high sensitivity to bending, we have successfully applied the device to detect the motions of finger (Figure S16a, Supporting Information) or wrist (Figure S16b, Supporting Information) bending, indicating the potential applications in human motion detection.

2.5. Human–Machine Interaction

Dynamic interaction between a machine and human are highly desired in artificial intelligence, service robots, and artificial limbs.[6,9] A fingertip of a wooden prosthetic hand attached with our MIG-based skin was employed to "feel" human touch. As shown in **Figure 5**a, when a human finger touches the prosthetic hand repeatedly, the touching could be detected by the flexible MIG-based skin. In addition, continuous and real-time detection of the pressure of a balloon was also conducted by grasping a balloon and gradually inflating or deflating the balloon. The signals show that when intermittently inflating, the pressure in the expanding balloon exhibits a series of fluctuations and the amplitude for the peaks gradually decreases as the balloon is expanding (Figure 5b). The deflating process is controlled with human hand by holding and releasing the outlet for several times and the sensor well reflects this process by showing stepwise signal (Figure 5c). Such subtle signal may not be perceived by our hands. Our demonstration is evidence that the flexible skins are useful in tactile sensing system for human–machine interaction and cognitive robots.

2.6. Spatial Distinguishing Ability of Sensors Array

The function of a single sensor is limited because it only detects the pressure of one "point". A two-dimensional sensors array can enable the mapping of pressures like real human skins.

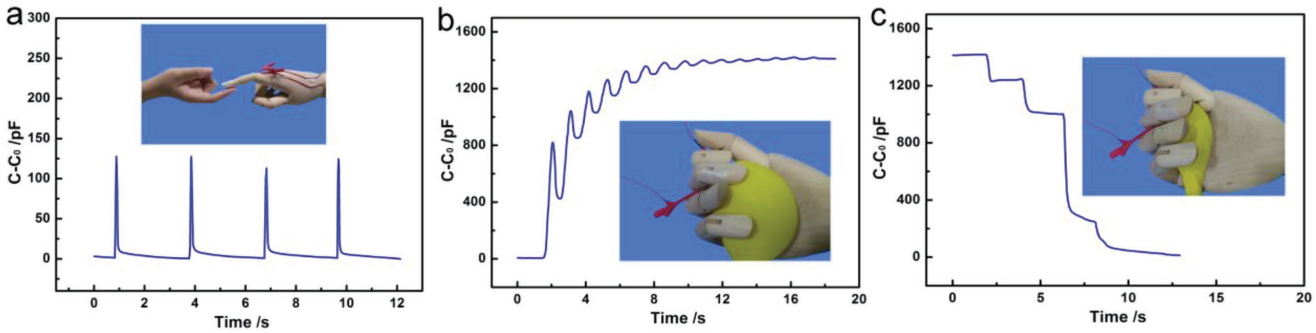

Figure 5. Applications of the flexible MIG-based skin. a) Real-time monitoring of capacitance variations from pressure arising by human finger touching on the sensor mounted on a wooden fingertip. Pressure sensing by holding a (b) deflating and (c) inflating balloon with an artificial hand.

The fabrication of the flexible MIG-based skin sensors array is schematically illustrated in **Figure 6**a (see the details in Experimental Section), showing a 5×5 capacitive parallel plate sensors array with sensors connected by laser-cut serpentine electrodes. The mapping of output capacitive signals could well match the PDMS stamp in the shape of "6" placed on the sensors array, as shown in Figure 6b. In addition, a square and a triangle of PDMS on the sensors array also induce the change of capacitance with corresponding shapes (Figure 6c). These results indicate that this device can be made to arrays and perform like our skin to map external pressures, and has the potential application in the wearable electronics and intelligent robots.

It should be noted that the capacitance of a pixel can be affected by the surrounding pixels in EDL-based sensors. However, we found that the crosstalk is only a weak effect that can be ignored in many applications. Our experiments show that when the top and bottom electrodes are not aligned (without overlap), the signal is ≈100 times weaker than the case with fully overlapped electrodes (see Figure S17, Supporting Information) at both 1 kHz and 1 MHz.

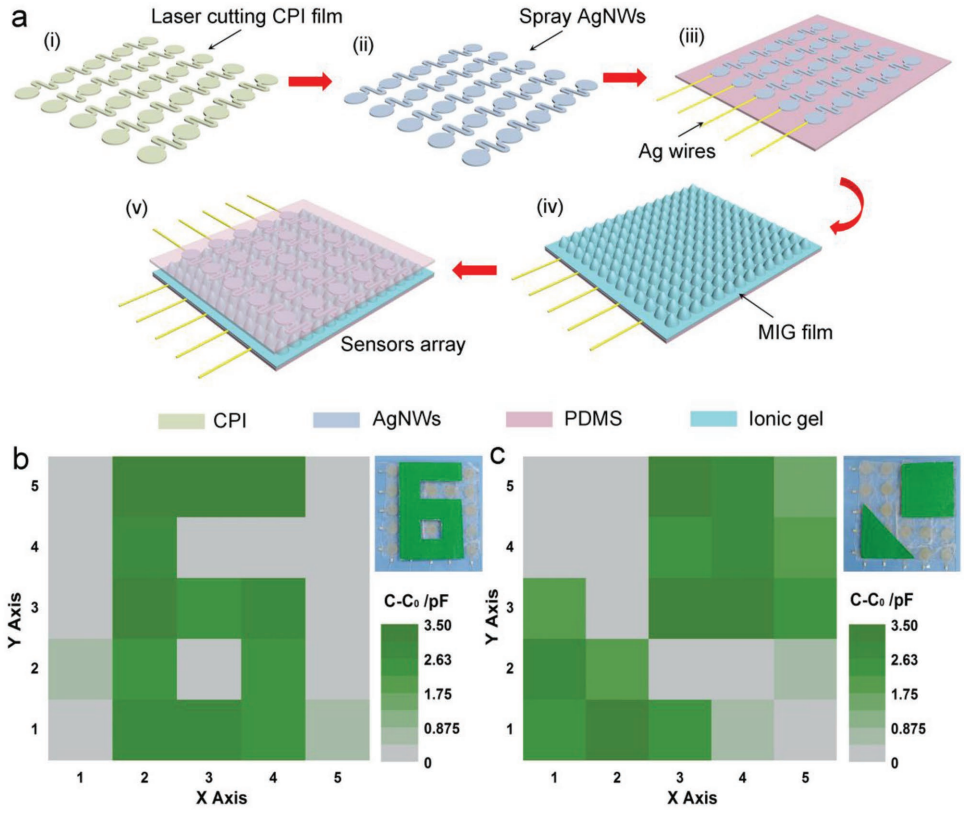

Figure 6. Spatial mapping of pressure. a) Schematic illustration for the fabrication of sensors array. i) Laser cutting CPI sheets into serpentine-shaped electrode frame. ii) Spraying silver nanowires on CPI frame to form serpentine-shaped electrode. iii) Pasting and patterning Ag electrode on PDMS substrate and embedding silver paste. iv) Placing the MIG dielectric layer on bottom electrodes. v) Sensors array. b) A PDMS stamp in the shape of "6" placed on the sensors array and corresponding mapping of the capacitance changes. c) A square- and a triangular-shaped PDMS plate on the skin and the corresponding capacitance signals.

3. Conclusion

In summary, we have used *Calathea zebrine* leaf to template ionic gel for high-performance flexible MIG-based skin. Owing to the remarkable EDL capacitance offered by microstructured MIG film, the flexible MIG-based skin shows an ultrahigh sensitivity of 54.31 kPa^{-1} in the pressure regime < 0.5 kPa and the sensitivity keeps > 1 kPa^{-1} over 0.1 Pa to 115 kPa, a pressure range over six orders of magnitude. The sensor also presents an ultralow LOD of 0.1 Pa, and a response time superior to that of human skin, and can be repeatedly tested for at least 5400 cycles. Such high-performance flexible MIG-based skin may enable sensitive tactile sensing in human–machine interaction, health and human activity monitoring, and so forth.

4. Experimental Section

Fabrication of Microstructured MIG Dielectric Layer: Fresh *Calathea zebrine* leaf was washed with deionized water for three times and then cut into a rectangle. Leaf edge was cut away to avoid inconsistency of the surface microstructures. After dried by air blowing, the *Calathea zebrine* rectangle was fixed on a glass substrate using taps. PDMS base (Sylgard 184, Dow Corning Co., Ltd) was mixed with the curing agent at a base to curing agent weight ratio of 5:1 and placed in a vacuum chamber at 25 °C for 20 min until bubbles disappeared. Next, the uncured PDMS was cast on the rectangular leaf. After curing at 70 °C for 1 h, it was peeled off as a second molding template. To reduce the undesired adhesion in the next second molding process, the molding template was exposed to air plasma treatment (TS-PL05, Dongxingaoke Co., Ltd) at 50 W for 1 min.

Two grams of P(VDF-HFP) (Sigma–Aldrich) was mixed in acetone (Sinopharm Chemical Reagent Co., Ltd) stirring for 2 h at room temperature. After adding 6 g of [EMIM][TFSI] (Sigma–Aldrich) into the polymer/solvent mixture, the solution was stirred for 30 min to mix completely. The ionic gel film was obtained by dropping the mixed polymer solution onto the PDMS second template and spinning coating the solution for 1 min at 2000 rpm to remove residual solvent from the ion gel. The weight ratio of P(VDF-HFP) and acetone was maintained at 1:10 for all preparation processes. The as-prepared ionic gel film was peeled off and cut to desired shapes. After these two molding process, a replica of the original surface, that is, the MIG film with positive pattern of *Calathea zebrine* leaf was fabricated, using directly as the dielectric layer.

Preparation of Flexible Electrode and Sensor: The synthesis of the ultrathin AgNWs can be seen in our previous report.[40] The AgNWs suspension was modified by the addition of water-soluble polymer hydroxypropylmethyl cellulose (HPMC, 0.5 wt%).[41] Spray coating was performed to prepare conductive AgNWs network by using an air gun (Badger) with a flow rate of AgNW solution of 6 $mL \cdot min^{-1}$. AgNWs were sprayed onto a CPI substrate and then dried at 70 °C for 10 min using as the top and bottom electrodes. Owing to the effect of HPMC, our AgNWs electrode exhibits strong adhesion to the substrate as well as low surface roughness. Subsequently, a silver wire was mounted on the terminal of the AgNWs film and heated at 80 °C for 1 h as contact. After that, the MIG film was sandwiched between two AgNWs films. As the MIG was quite thin (40 µm in total) and sticky, the flat surface of the MIG spontaneously adhered to the bottom electrode when slowly placed on the electrode and an extra pressure was applied to remove the air gap and further increase the interfacial strength. Finally the edges of the device were bonded with 3M Scotch tape. The size of the devices was typically 1.5 cm^2 with an initial capacitance of ≈10 pF.

Fabrication of Sensors Array: 5 × 5 sensors connected with serpentines were cut by using a CO_2 laser cutter (WE-6040) and followed by ultrasonication in deionized water and alcohol in sequence. Subsequently, AgNWs were sprayed on the patterned CPI. After that the AgNWs/CPI electrodes were pasted on PDMS and connected with silver wires using silver paste. Next, MIG dielectric layers were mounted on the AgNWs/CPI/PDMS bottom electrode and another AgNWs/CPI/PDMS top electrode with the same size was placed orthogonally to the MIG/AgNWs/CPI/PDMS film face to face, forming a sandwiched structure. The device fabrication is presented in Figure 6a.

Characterization and Measurements: The microstructures of the *Calathea zebrine* leaf, PDMS molding templates, and MIG film were inspected by field-emission SEM (TESCAN) operated at 5 kV. Note that the *Calathea zebrine* leaf was pretreated by critical point drying (EM CPD300, LEICA) before SEM characterization to avoid wrinkling during dying. The statistical distribution of the microcones was obtained by using software (Nano Measurer 1.2). The stress–strain curve of the MIG film was tested by using a Micro-nano extensometer (UTM 150, KEYSIGHT). An Inductance Capacitance and Resistance meter (E4980AL, KEYSIGHT) was used to measure the capacitance of the sensor at a testing frequency of ≈1 MHz, if not specified. A force gauge with a computer-controlled stage (XLD-20E, Jingkong Mechanical testing Co., Ltd) was used to record the external pressure. The sensors were placed on the testing system for cyclic compression/release tests at a constant speed of 2 mm min^{-1}. Besides, the electrical signal was recorded by repeatedly applying and releasing a constant pressure. For the bending test, a device was clamped on a home-made flexibility tester and subjected to different bending radii. The capacitance of all sensors in this work has been correlated with pressure by a standard machine.

Supporting Information

Supporting Information is available from the Wiley Online Library or from the author.

Acknowledgements

Z.Q. and Y.W. contributed equally to this work. This work was financially supported by the funds of the "Guangdong Innovative and Entrepreneurial Research Team Program" under contract no. 2016ZT06G587, the National Natural Science Foundation of China (nos U1613204 and 51771089), the "Science Technology and Innovation Committee of Shenzhen Municipality" (grant no. JCYJ20170817111714314 and JCYJ20160613160524999), and the "Peacock Plan" (no. Y01256120).

Conflict of Interest

The authors declare no conflict of interest.

Keywords

electric double layers, flexible electronic skin, microstructured ionic gels, pressure sensors

Received: April 5, 2018
Revised: June 17, 2018
Published online: July 27, 2018

[1] S. C. B. Mannsfeld, B. C. K. Tee, R. M. Stoltenberg, C. V. H. H. Chen, S. Barman, B. V. O. Muir, A. N. Sokolov, C. Reese, Z. Bao, *Nat. Mater.* **2010**, *9*, 859.
[2] M. L. Hammock, A. Chortos, B. C. K. Tee, J. B. H. Tok, Z. Bao, *Adv. Mater.* **2013**, *25*, 5997.

[3] Y. Wang, L. Wang, T. Yang, X. Li, X. Zang, M. Zhu, K. Wang, D. Wu, H. Zhu, *Adv. Funct. Mater.* **2014**, *24*, 4666.
[4] Y. Zang, F. Zhang, C.-A. Di, D. Zhu, *Mater. Horiz.* **2015**, *2*, 140.
[5] X. D. Wang, L. Dong, H. L. Zhang, R. M. Yu, C. F. Pan, Z. L. Wang, *Adv. Sci.* **2015**, *2*, 1500169.
[6] T. Yang, D. Xie, Z. Li, H. Zhu, *Mater. Sci. Eng. R-Rep.* **2017**, *115*, 1.
[7] X. Zhao, Q. Hua, R. Yu, Y. Zhang, C. Pan, *Adv. Electron. Mater.* **2015**, *1*, 1500142.
[8] Y. Wan, Y. Wang, C. F. Guo, *Mater. Today Phys.* **2017**, *1*, 61.
[9] H. Ding, X. Yang, N. Zheng, M. Li, Y. Lai, H. Wu, *Natl. Sci. Rev.* **2018**, https://doi.org/10.1093/nsr/nwx148.
[10] S. Kang, J. Lee, S. Lee, S. Kim, J.-K. Kim, H. Algadi, S. Al-Sayari, D.-E. Kim, D. Kim, T. Lee, *Adv. Electron. Mater.* **2016**, *2*, 1600356.
[11] J. Park, Y. Lee, J. Hong, M. Ha, Y. D. Jung, H. Lim, S. Y. Kim, H. Ko, *ACS Nano* **2014**, *8*, 4689.
[12] Q. L. Hua, H. T. Liu, J. Zhao, D. F. Peng, X. N. Yang, L. Gu, C. F. Pan, *Adv. Electron. Mater.* **2016**, *2*, 1600093.
[13] Q. Hua, J. Sun, H. Liu, R. Bao, R. Yu, J. Zhai, C. Pan, Z. L. Wang, *Nat. Commun.* **2018**, *9*, 244.
[14] D. J. Lipomi, M. Vosgueritchian, B. C. K. Tee, S. L. Hellstrom, J. A. Lee, C. H. Fox, Z. Bao, *Nat. Nanotechnol.* **2011**, *6*, 788.
[15] T. Li, H. Luo, L. Qin, X. Wang, Z. Xiong, H. Ding, Y. Gu, Z. Liu, T. Zhang, *Small* **2016**, *12*, 5042.
[16] Y. Joo, J. Yoon, J. Ha, T. Kim, S. Lee, B. Lee, C. Pang, Y. Hong, *Adv. Electron. Mater.* **2017**, *3*, 1600455.
[17] W. Wu, X. Wen, Z. L. Wang, *Science* **2013**, *340*, 952.
[18] Z. F. Chen, Z. Wang, X. M. Li, Y. X. Lin, N. Q. Luo, M. Z. Long, N. Zhao, J. B. Xu, *ACS Nano* **2017**, *11*, 4507.
[19] C. Dagdeviren, Y. Su, P. Joe, R. Yona, Y. Liu, Y.-S. Kim, Y. Huang, A. R. Damadoran, J. Xia, L. W. Martin, Y. Huang, J. A. Rogers, *Nat. Commun.* **2014**, *5*, 4496.
[20] F.-R. Fan, L. Lin, G. Zhu, W. Wu, R. Zhang, Z. L. Wang, *Nano Lett.* **2012**, *12*, 3109.
[21] Z. Lin, J. Chen, X. Li, Z. Zhou, K. Meng, W. Wei, J. Yang, Z. L. Wang, *ACS Nano* **2017**, *11*, 8830.
[22] B. Q. Nie, R. Y. Li, J. Cao, J. D. Brandt, T. R. Pan, *Adv. Mater.* **2015**, *27*, 6055.
[23] S. Chen, B. Zhuo, X. Guo, *ACS Appl. Mater. Interfaces* **2016**, *8*, 20364.
[24] S. Chen, K. Jiang, Z. Lou, D. Chen, G. Z. Shen, *Adv. Mater. Technol.* **2018**, *31*, 700248.
[25] B. Q. Nie, S. Y. Xing, J. D. Brandt, T. R. Pan, *Lab Chip* **2012**, *12*, 1110.
[26] K. H. Lee, M. S. Kang, S. Zhang, Y. Gu, T. P. Lodge, C. D. Frisbie, *Adv. Mater.* **2012**, *24*, 4457.
[27] Y. Wang, S. Gong, S. J. Wang, G. P. Simon, W. Cheng, *Mater. Horiz.* **2016**, *3*, 208.
[28] S. H. Cho, S. W. Lee, S. Yu, H. Kim, S. Chang, D. Kang, I. Hwang, H. S. Kang, B. Jeong, E. H. Kim, S. M. Cho, K. L. Kim, H. Lee, W. Shim, C. Park, *ACS Appl. Mater. Interfaces* **2017**, *9*, 10128.
[29] K. Koch, W. Barthlott, *Phil. Trans. R. Soc. A* **2009**, *367*, 1487.
[30] D. Qin, Y. N. Xia, G. M. Whitesides, *Nat. Protoc.* **2010**, *5*, 491.
[31] J. Lee, H. Kwon, J. Seo, S. Shin, J. H. Koo, C. Pang, S. Son, J. H. Kim, Y. H. Jang, D. E. Kim, T. Lee, *Adv. Mater.* **2015**, *27*, 2433.
[32] Y. Joo, J. Byun, N. Seong, J. Ha, H. Kim, S. Kim, T. Kim, H. Im, D. Kim, Y. Hong, *Nanoscale* **2015**, *7*, 6208.
[33] S. Yao, Y. Zhu, *Nanoscale* **2014**, *6*, 2345.
[34] B. You, C. J. Han, Y. Kim, B. K. Ju, J. W. Kim, *J. Mater. Chem. A* **2016**, *4*, 10435.
[35] A. Chortos, Z. Bao, *Mater. Today* **2014**, *17*, 321.
[36] Z. X. Tang, L. E. Scriven, H. T. Davis, *J. Chem. Phys.* **1992**, *97*, 494.
[37] C. Keplinger, J. Y. Sun, C. C. Foo, P. Rothemund, G. M. Whitesides, Z. G. Suo, *Science* **2013**, *341*, 984.
[38] K. B. Oldham, *J. Electroanal. Chem.* **2008**, *613*, 131.
[39] G. Schwartz, B. C. K. Tee, J. G. Mei, A. L. Appleton, D. H. Kim, H. L. Wang, Z. Bao, *Nat. Commun.* **2013**, *4*, 1859.
[40] Y. Wan, Z. Qiu, Y. Hong, Y. Wang, J. Zhang, Q. Liu, Z. Wu, C. F. Guo, *Adv. Electron. Mater.* **2018**, *4*, 1700586.
[41] F. Hoeng, A. Denneulin, N. Reverdy-Bruas, G. Krosnicki, J. Bras, *Appl. Surf. Sci.* **2017**, *394*, 160.